Synlett O. Kwon et al. Cluster

Development of 3,5-Di-*tert*-butylphenol as a Model Substrate for Biomimetic Aerobic Copper Catalysis

Ohhyeon Kwon[a]
Kenneth Virgel N. Esguerra[a]
Michael Glazerman †[b]
Laurène Petitjean[a]
Yalun Xu[a]
Xavier Ottenwaelder[b]
Jean-Philip Lumb *[a]

[a] Department of Chemistry, McGill University, 801 Sherbrooke Street West, Montreal, Quebec, H3A 0B8, Canada
jean-philip.lumb@mcgill.ca
[b] Department of Chemistry and Biochemistry, Concordia University, 7141 Sherbrooke Street West, Montreal, Quebec, H3A 0B8, Canada
dr.x@concordia.ca

† In memoriam

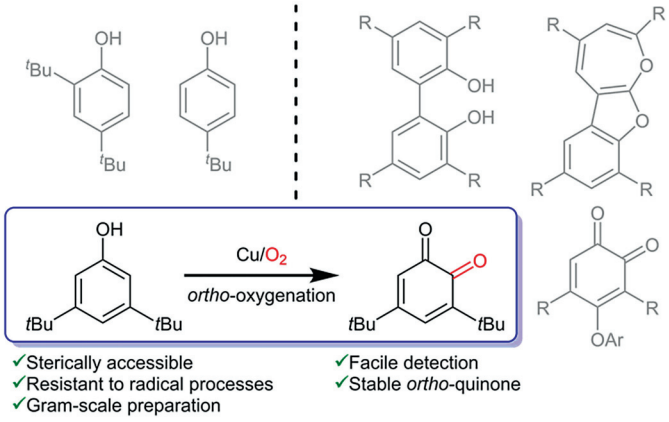

Received: 17.01.2017
Accepted after revision: 28.02.2017
Published online:
DOI: 10.1055/s-0036-1588761; Art ID: st-2017-r0048-c

Abstract We develop 3,5-di-*tert*-butylphenol as a strategic substrate for the evaluation of biomimetic Cu_2–O_2 complexes intended to mimic the activity of tyrosinase. We describe a practical and scalable synthesis and validate its use in an aerobic *ortho*-oxygenation catalyzed by *N*,*N*′-di-*tert*-butylethylenediamine and $[Cu(CH_3CN)_4]PF_6$.

Key words aerobic oxidation, biomimetic catalysis, copper, dearomatization, tyrosinase, oxidative coupling, oxepinobenzofuran

Aerobic catalysis has garnered considerable interest as a means of driving chemical synthesis from a renewable source of energy.[1] Molecular oxygen (O_2) is abundant and nontoxic, and its use as a terminal oxidant is atom-economic and benign in instances where H_2O is generated as the sole, stoichiometric byproduct.[2] While attractive, these features are often offset by challenges of controlling chemo-, regio- and stereoselectivity, particularly in complex molecule settings.[1b] The triplet electronic ground state of O_2 often mandates high activation energies for direct reaction with organic molecules in the absence of light or a transition-metal catalyst,[3] and selectivity is often diminished by radical-based mechanisms of oxidation.[4]

Metalloenzymes offer a unique source of inspiration with which to overcome these challenges, since many enzyme-mediated aerobic oxidations exhibit exquisite levels of selectivity.[1a,5] Discrete metal complexes aimed to mimic these systems have provided insight into many of the requirements for selective O_2 activation and substrate oxidation.[6] These simplified model systems recreate the protein active sites in the absence of a supporting amino acid matrix,[7] which facilitates the use of non-natural substrates under reaction conditions more suitable for organic synthesis (i.e., organic solvents and elevated or cryogenic temperatures). While such bioinspired catalysts are attractive, few have successfully mimicked the catalytic activity of metalloenzymes and are generally not translatable to practical and scalable protocols that are applicable for synthesis.[1a,8] We have been particularly interested in mimics of the enzyme tyrosinase, which is a ubiquitous, dinuclear copper (Cu)-containing metalloenzyme that triggers the synthesis of melanin pigments by catalyzing the selective *ortho*-oxygenation of L-tyrosine to L-dopaquinone (Scheme 1, a).[8] Tyrosinase has been the focus of numerous, bioinorganic studies, which have led to a number of small-molecule enzyme mimics that faithfully recreate the enzyme's ability to (1) activate O_2 as a characteristic side-on μ-η^2:η^2 peroxo complex, and (2) oxygenate exogenous phenolic substrates.[7–9] The overwhelming majority of these studies have been conducted under stoichiometric conditions, in which a preformed phenolate is added to a preformed $L_nCu_2O_2$ complex at low temperatures, under conditions that are not amenable to catalysis.[2a,10] Under more catalytically relevant conditions that employ phenols instead of phenolates at room temperature, more complex reaction mixtures at incomplete conversions are obtained, owing to competitive radical-based oxidations that are not observed for tyrosinase itself (Scheme 1, b).[2a,7a]

A significant complication in the advancement and development of tyrosinase mimics has been the inherent reactivity of the *ortho*-quinone products. *ortho*-Quinones readily engage in a range of transformations that can include addition, condensation, and redox reactions, as well

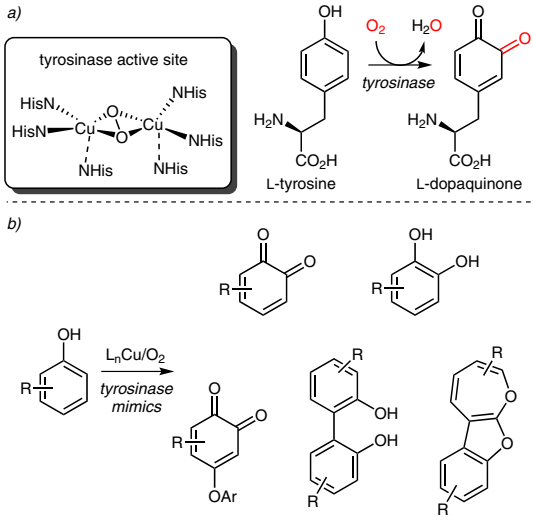

Scheme 1 a) Tyrosinase-mediated *ortho*-oxygenation of L-tyrosine. b) Copper-mediated catalytic aerobic oxidation of phenols by small-molecule tyrosinase mimics.

as cycloadditions.[11] Moreover, *ortho*-quinones are good ligands for Cu(I),[12] complicating the delicate coordination chemistry that must be preserved in order to selectively activate O_2 as the side-on μ-η^2:η^2 peroxo complex. Historically, many of these challenges have been addressed by using 2,4-di-*tert*-butylphenol (**1**) as a model substrate, since its corresponding *ortho*-quinone, 3,5-di-*tert*-butyl-*ortho*-benzoquinone (**2**) is relatively stable (Equation 1).[13] However, the use of **1** is complicated by the very same properties that impart stability to **2**. Namely, the steric shielding of the *tert*-butyl substituent at C2, near the coordinating O atom, makes an inner-sphere mechanism of oxygenation difficult, especially given the often sterically demanding ligands used to mimic the tyrosinase core. In addition, the electron-donating properties of the *tert*-butyl substituents in the *ortho* and *para* positions make phenol **1** a relatively easy phenol to oxidize (E^{ox} = 1.48 V vs. SCE in CH_2Cl_2, see SI) because the 2,4-substitution pattern can help to stabilize the phenoxyl radical.[14] As a result, **1** is prone to a range of radical-based reactions, in what is best described as non-tyrosinase-like oxidations.[5g]

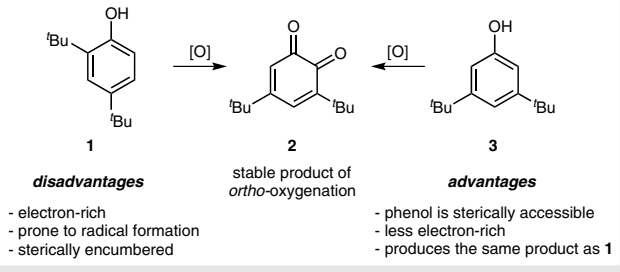

Equation 1 *ortho*-Oxygenation of two regioisomers of di-*tert*-butylphenol **1** and **3**

Recognizing these challenges, we report the use of 3,5-di-*tert*-butylphenol (**3**) as a strategic alternative to **1** for probing the reactivity of tyrosinase mimics. Benefits of **3** include a higher redox potential (E^{ox} = 1.62 V vs. SCE in CH_2Cl_2, see Supporting Information) relative to **1**, consistent with a *meta* disposition of the *tert*-butyl groups, as well as a minimized steric profile. In addition, *ortho*-oxygenation of **3** still provides *ortho*-quinone **2**, benefiting from the relative stability discussed above. To our knowledge, phenol **3** has not been previously evaluated as a substrate for tyrosinase mimics.[15] Here, we trace its development, synthesis, and optimization in the context of our groups' program in tyrosinase mimicry.

Our motivations to develop phenol **3** stem from our recently reported conditions for the *ortho*-oxygenation of phenols that employ catalytic quantities of $[Cu(CH_3CN)_4]PF_6$ (abbreviated as $CuPF_6$) in conjunction with *N*,*N*′-di-*tert*-butylethylenediamine (DBED) and O_2 (Scheme 2).[5g] Under these conditions, 4-*tert*-butylphenol (**4**) is cleanly converted into coupled *ortho*-quinone **6** (>95% yield) after four hours at room temperature, in a process that is composed of (*i*) a relatively fast *ortho*-oxygenation of **4** into DBED/Cu(II)-semiquinone (**5**), followed by (*ii*) a relatively slow oxidative C–O coupling to provide **6**. By monitoring the reaction at low temperatures (−120 °C to −80 °C), we successfully investigated the O_2 activation and oxygen-atom transfer steps leading to **5**, which are consistent with a tyrosinase-like mechanism.[16] However, under these conditions, Cu is not released from **5**, preventing a detailed mechanistic analysis of the turnover step. At elevated temperatures, where turnover does occur, step (*ii*) is rate limiting, complicating the mechanistic picture. Most notably, **6** is not observed when phenol **4** is oxygenated with tyrosinase.[17]

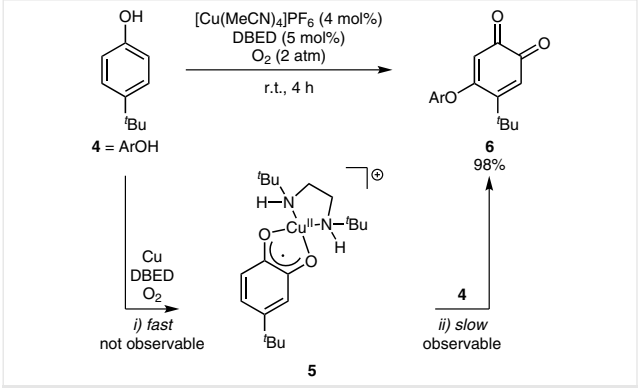

Scheme 2 Simplified mechanism for the Cu/DBED-catalyzed aerobic oxidation of 4-*tert*-butylphenol (**4**)

Because quinone **2** (cf. Equation 1) does not undergo oxidative coupling as described in step (*ii*) due to steric constraints, the *ortho*-oxygenation of **1** to **2** would offer a more tractable system for mechanistic investigations. However, **1** is selectively oxidized into oxepinobenzofuran **7** by the

$CuPF_6$/DBED system (Scheme 3, a).[5g] The occurrence of oxepinobenzofurans related to **7** as a product of metal-mediated phenol oxidation can be traced to the earliest work of Müller and coworkers in 1961,[18] who originally assigned its structure as benzoxete **7′**. This structure has persisted in the literature,[2a] despite a structural reassignment by Hitchcock in 1978,[19] and others based on theoretical calculations,[20] or spectroscopic data.[21] We present here an X-ray structure for **7**, along with phenyl-substituted derivative **7a** (Scheme 3, b),[22] which substantiates Meier's structural revision, as well as the detailed characterization conducted in 2013 by Limberg.[21c]

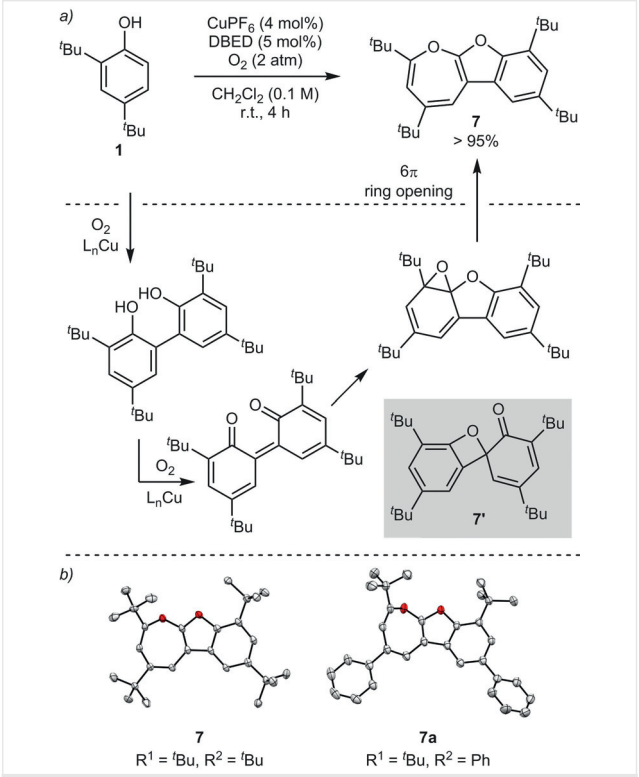

Scheme 3 a) A concise mechanism of the Cu-catalyzed aerobic oxidation of phenol **1** to the oxepinobenzofuran **7**. b) ORTEP views at 50% ellipsoid probability of **7** and derivative **7a** in their crystal structures, with hydrogen atoms removed for clarity.

Recognizing the complications associated with **1** and **4** as probes for the evaluation of $L_nCu_2O_2$ complexes, we considered phenol **3** as a strategic alternative. Although commercially available,[23] the high cost of **3** prompted us to develop a concise and scalable route that could provide **3** in suitably pure form for mechanistic studies. Initially, we were drawn to Stahl's recently reported conditions for the synthesis of *meta*-substituted phenols by oxidative condensation of simple carbonyl compounds.[24] Adapting these conditions to the synthesis of **3** began by a base-mediated aldol condensation of pivaldehyde and pinacolone, followed by annulation with acetone, and catalytic aerobic dehydrogenation to provide **3** (Table 1). Efforts to optimize this process surveyed $Pd(OAc)_2$ and $Pd(TFA)_2$ as sources of Pd (Table 1, entries 1 and 2), as well as prolonged reaction times (Table 1, entry 3) and increased temperatures (Table 1, entry 4). Unfortunately, none of these changes significantly improved reaction efficiency. It was only upon doubling the catalyst loading that we observed a statistically significant increase in the yield of **3** (Table 1, entry 5), which appeared to plateau at 25 mol% of $Pd(TFA)_2$, 25 mol% of the amino pyridine ligand (2-(*N*,*N*-dimethylamino)pyridine), and 50 mol% of the sulfonic acid (Table 1, entry 6). By prolonging the reaction time under these conditions, we were able to increase the yield of **3** to >40% after 48 or 72 hours at 120 °C (Table 1, entries 7 and 8). Using these optimized conditions, **3** was prepared in 47% overall yield after purification on gram scale, starting from the corresponding ketone and aldehyde precursors (Scheme 4). While this pathway is conceptually attractive, our inability to improve the efficiency of this dehydrogenation, particularly at the elevated catalyst loadings, led us to consider alternative approaches to **3**.

Table 1 Initial Route for the Preparation of 3,5-Di-*tert*-butylphenol **3** and the Optimization of the Palladium-Catalyzed Dehydrogenative Aromatization

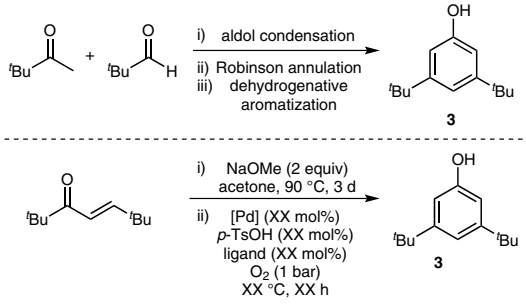

Entry	[Pd] (mol%)	Ligand (mol%)[a]	*p*-TsOH (mol%)	Temp (°C)	Time (h)	Conversion (%)	Yield (%)[b]
1	$Pd(OAc)_2$ (5)	10	10	80	24	44	13
2	$Pd(TFA)_2$ (5)	10	10	80	24	47	16
3	$Pd(TFA)_2$ (5)	10	10	80	48	62	18
4	$Pd(TFA)_2$ (5)	10	10	120	24	68	21
5	$Pd(TFA)_2$ (10)	10	25	120	24	64	37
6	$Pd(TFA)_2$ (25)	25	50	120	24	69	41
7	$Pd(TFA)_2$ (25)	25	50	120	48	70	43
8	$Pd(TFA)_2$ (25)	25	50	120	72	71	46

[a] Ligand = 2-(*N*,*N*-dimethylamino)pyridine.
[b] Conversion and yield based on recovered starting material and product following purification.

We decided to prepare **3** from 1-bromo-3,5-di-*tert*-butylbenzene (**8**), which is commercially available or easily prepared (see Supporting Information). While the one-step hydroxylation of aryl halides has recently received consid-

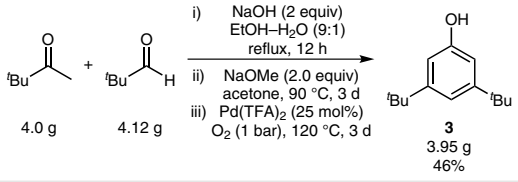

Scheme 4 Gram-scale preparation of phenol **3** via oxidative condensation starting from pivaldehyde and pinacolone

erable attention,[25] application of existing methodologies to **8** under a range of Cu-mediated coupling conditions with hydroxide led to disappointing results (Table 2). These include conventional cross-coupling methodologies by Xia and coworkers as well as Chen and coworkers (Table 2, entries 1 and 2),[25a,b] and biphasic conditions employing water as the solvent and a range of phase-transfer catalysts, reported by Chen (Table 2, entry 3)[25c] and Wang (Table 2, entry 4).[25d] We did find, however, that conditions initially reported by Elder and co-workers,[25e] involving hydroxylation of **8** with H_2O and substoichiometric quantities of Cu metal and cupric oxide, returned **3** in 74% yield, after heating in an autoclave at 275 °C for 36 hours (Table 2, entry 5). Unfortunately, practical limitations precluded large-scale development. Finally, we settled on an alternative, two-step approach to **3**, relying first on the conversion of aryl bromide **8** into the corresponding boronic ester by way of the Grignard reagent, followed by oxidation using Oxone® under conditions reported by Maleczka and coworkers (Table 2, entry 6).[26] This route has proven to be reproducible on 100 mmol scale, providing **3** as a white solid in 80% yield following recrystallization from hexanes.[27] A single X-ray crystal structure of **3** was obtained, and is provided in Scheme 5.[22] We note that in their initial publication,[26] Maleczka and coworkers express caution to the use of Oxone® on large scales. While we have not experienced any difficulties, we likewise stress the importance of adding the oxidant with care.

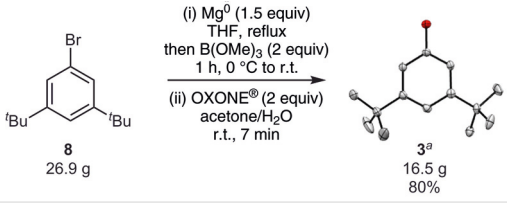

Scheme 5 Decagram-scale synthesis of phenol **3** via borylation/oxidation of **8**. [a] ORTEP of one of three independent molecules of **3** at 50% ellipsoid probability. Hydrogen atoms were omitted for clarity. See Supporting Information for more details.

With a synthetic route to **3** secured, we evaluated its performance as a model substrate for *ortho*-oxygenation using our $CuPF_6$/DBED system (Table 3).[9e] Gratifyingly, exposure of **3** to our previously optimized conditions provides quinone **2** after four hours at room temperature, albeit at incomplete conversion with a loss of mass balance of ca. 10% (Table 3, entry 1). While higher loadings of DBED provided marginal improvements (Table 3, entry 2), the reaction's incomplete conversion prompted us to evaluate $MgSO_4$ as an additive. We have previously demonstrated that a desiccant, such as $MgSO_4$, can improve reaction efficiency,[9e] but no benefits were observed in the current context at both 5 and 10 mol% loadings of DBED (Table 3, entries 3 and 4). Ultimately, clean conditions, proceeding to complete conversion of **3**, were realized by increasing the Cu loading to 8 mol%, and using either 15 or 20 mol% of DBED, which returns NMR yields of **2** in excess of 95% (Table

Table 2 Hydroxylation of 1-Bromo-3,5-di-*tert*-butylbenzene (**8**) to Phenol **3**

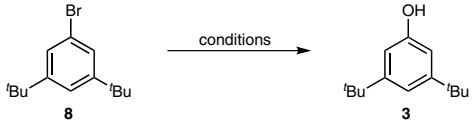

Entry	Conditions[a]	Yield (%)[b]
1	$Cu(acac)_2$ (0.5 mol%), **L5** (0.5 mol%), $LiOH·H_2O$ (2.1 equiv), DMSO–H_2O (4:1, 0.1 M), 80 °C, 24 h[25a]	–[c]
2	$Cu(8\text{-HQ})_2$ (10 mol%), NaOH (30% in H_2O), 110 °C, 24 h[25b]	–[c]
3	CuI (10 mol%), KOH (6.0 equiv), PEG-400–H_2O (4:1), 120 °C, 8 h[25c]	–[c]
4	Cu_2O (5 mol%), **L** (10 mol%), TBAOH (1 mL/0.5 mmol), H_2O, 110 °C, 24 h[25d]	–[c]
5	Cu^0 (20 mol%), CuO (50 mol%), NaOH (6.67 equiv), H_2O, 275 °C, 36 h[25e]	74[d]
6	i) Mg^0 (1.5 equiv), THF, reflux, then $B(OMe)_3$ (2 equiv), 1 h, 0 °C to r.t. ii) Oxone® (2 equiv), acetone–H_2O, r.t., 7 min[26]	80[e]

[a] For detailed procedures and ligand structures, see Supporting Information.
[b] Isolated yields.
[c] TLC analysis showed little to no conversion of starting material due in part to issues of solubility.
[d] Isolated yield before recrystallization.
[e] Isolated yield after recrystallization.

3, entries 5 and 6). Yields remain consistently high on scales of up to 10 grams (Table 3, entry 7), and most importantly, oxidation byproducts are not detected in significant amounts (< 5%) over the course of the reaction (see Figures S1 and S2 in the Supporting Information).

Table 3 Optimization of the Cu/DBED-Catalyzed Aerobic *ortho*-Oxygenation of 3,5-Di-*tert*-butylphenol (**3**)

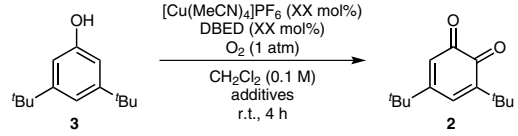

Entry	Cu loading (mol%)	DBED (mol%)	Additive (equiv)	Conversion (%)	Yield (%)[a]
1	4	5	–	84	76
2	4	10	–	80	78
3	4	5	$MgSO_4$ (3)	60	55
4	4	10	$MgSO_4$ (3)	80	71
5	8	15	–	99	95
6	8	20	–	99	95
7[b]	8	15	–	–	97[c]

[a] ^{1}H-NMR conversions and yields calculated using hexamethylbenzene as the internal standard.
[b] Reaction performed on 10 g of phenol.
[c] Isolated yield.

In previous mechanistic studies from Stack's group and our own groups,[9c,d,16] DBED/Cu(I) was shown to self-assemble into a μ-η^2:η^2 peroxodicopper(II) species when exposed to O_2 that is spectroscopically similar to the active site of tyrosinase. However, in each of these previous studies, limitations of the substrates used to evaluate the reactivity of this biomimetic oxidant precluded a detailed mechanistic investigation under catalytic conditions. In Stack's studies, the phenolate anion of **1** was shown to undergo stoichiometric *ortho*-oxygenation to a mixture of **2** and 3,5-di-*tert*-butylcatechol, and we have shown that **1** undergoes a radical-based oxidation under catalytic conditions to provide **7**.[5g] Removing the 2-*tert*-butyl substituent, as in **4**, does lead to more efficient catalysis for the oxygenation step,[9e] but at the expense of a supplementary oxidative coupling step (Scheme 2). Hence, the substrates used to evaluate the reactivity of this biomimetic oxidant precluded a detailed mechanistic investigation under true catalytic conditions, leaving many fundamentally important questions unanswered. In this manuscript, we have provided a rationale for developing 3,5-di-*tert*-butylphenol (**3**) as a strategic alternative and have validated its suitability for *ortho* oxygenation under our biomimetic reaction conditions. Most notably, the oxygenation of **3** proceeds to a single product at complete conversion of the substrate in reaction times that are suitable for mechanistic work, aimed at elucidating key events in a catalytic mimic of tyrosinase, which remains an unsolved challenge. Detailed insight into this catalytic process should facilitate the translation of fundamental, bioinorganic studies into more practical, catalytic aerobic processes of synthetic value, as has been observed for related, bioinspired aerobic oxidations of alcohols.[28] Given the breadth of biomimetic metal complexes, we anticipate a number of applications for **3** beyond tyrosinase, in cases where an inner-sphere substrate oxidation is desired.

Acknowledgment

Financial support was provided by the Natural Sciences and Engineering Council of Canada (NSERC, Discovery Grants to J.-P.L. and X.O.), the Fonds de Recherche du Québec – Nature et Technologies (FRQNT, Team Grant to J.-P.L.), the FRQNT Centre for Green Chemistry and Catalysis at McGill University, the NSERC CREATE Program in Green Chemistry at McGill University, and the McGill University-Canadian Institutes of Health Drug Development Trainee Program (doctoral fellowship to K.V.N.E.). We are grateful to Farshid Effaty (Concordia University) for help with the electrochemical measurements.

Supporting Information

Supporting information for this article is available online at http://dx.doi.org/10.1055/s-0036-1588761.

References and Notes

(1) (a) Que, L.; Tolman, W. B. *Nature (London, U.K.)* **2008**, *455*, 333. (b) McCann, S. D.; Stahl, S. S. *Acc. Chem. Res.* **2015**, *48*, 1756.
(2) (a) Allen, S. E.; Walvoord, R. R.; Padilla-Salinas, R.; Kozlowski, M. C. *Chem. Rev.* **2013**, *113*, 6234. (b) Schultz, M. J.; Sigman, M. S. *Tetrahedron* **2006**, *62*, 8227. (c) Wendlandt, A. E.; Suess, A. M.; Stahl, S. S. *Angew. Chem. Int. Ed.* **2011**, *50*, 11062. (d) Campbell, A. N.; Stahl, S. S. *Acc. Chem. Res.* **2012**, *45*, 851. (e) Zhang, C.; Tang, C.; Jiao, N. *Chem. Soc. Rev.* **2012**, *41*, 3464. (f) Shi, Z.; Zhang, C.; Tang, C.; Jiao, N. *Chem. Soc. Rev.* **2012**, *41*, 3381. (g) Gulzar, N.; Schweitzer-Chaput, B.; Klussmann, M. *Catal. Sci. Technol.* **2014**, *4*, 2778.
(3) Roduner, E.; Kaim, W.; Sarkar, B.; Urlacher, V. B.; Pleiss, J.; Gläser, R.; Einicke, W.-D.; Sprenger, G. A.; Beifuß, U.; Klemm, E.; Liebner, C.; Hieronymus, H.; Hsu, S.-F.; Plietker, B.; Laschat, S. *ChemCatChem* **2013**, *5*, 82.
(4) Altwicker, E. R. *Chem. Rev.* **1967**, *67*, 475.
(5) For selected reviews and references of aerobic alcohol and amine oxidations, see: (a) Ryland, B. L.; Stahl, S. S. *Angew. Chem. Int. Ed.* **2014**, *53*, 8824. (b) Chen, B.; Wang, L.; Gao, S. *ACS Catal.* **2015**, *5*, 5851. (c) Steves, J. E.; Stahl, S. S. *J. Org. Chem.* **2015**, *80*, 11184. (d) Stahl, S. S.; Alsters, P. L. *Liquid Phase Aerobic Oxidation Catalysis: Industrial Applications and Academic Perspectives*; Wiley-VCH: Weinheim, **2016**. (e) Xu, B.; Hartigan, E. M.; Feula, G.; Huang, Z.; Lumb, J.-P.; Arndtsen, B. A. *Angew. Chem. Int. Ed.* **2016**, *55*, 15802. For selected examples of enzyme-inspired selective aerobic oxidations, see: (f) Hoover, J. M.; Stahl, S. S. *J. Am. Chem. Soc.* **2011**, *133*, 16901. (g) Esguerra, K. V. N.; Fall, Y.; Petitjean, L.; Lumb, J.-P. *J. Am. Chem. Soc.* **2014**, *136*, 7662. (h) Lee, Y. E.; Cao, T.; Torruellas, C.; Kozlowski, M. C. *J. Am. Chem. Soc.* **2014**, *136*, 6782.

(6) Solomon, E. I.; Heppner, D. E.; Johnston, E. M.; Ginsbach, J. W.; Cirera, J.; Qayyum, M.; Kieber-Emmons, M. T.; Kjaergaard, C. H.; Hadt, R. G.; Tian, L. *Chem. Rev.* **2014**, *114*, 3659.
(7) (a) Rolff, M.; Schottenheim, J.; Decker, H.; Tuczek, F. *Chem. Soc. Rev.* **2011**, *40*, 4077. (b) Hamann, J. N.; Herzigkeit, B.; Jurgeleit, R.; Tuczek, F. *Coord. Chem. Rev.* **2017**, *334*, 54.
(8) (a) Sugumaran, M. *FEBS Lett.* **1991**, *295*, 233. (b) Mahadevan, V.; Gebbink, R. J. M. K.; Stack, T. D. P. *Curr. Opin. Chem. Biol.* **2000**, *4*, 228. (c) Simon, J. D.; Peles, D.; Wakamatsu, K.; Ito, S. *Pigm. Cell Melanoma Res.* **2009**, *2*, 563. (d) Loizzo, M. R.; Tundis, R.; Menichini, F. *Compr. Rev. Food Sci. Food Saf.* **2012**, *11*, 378.
(9) (a) Reglier, M.; Jorand, C.; Waegell, B. *J. Chem. Soc., Chem. Commun.* **1990**, 1752. (b) Battaini, G.; Carolis, M. D.; Monzani, E.; Tuczek, F.; Casella, L. *Chem. Commun.* **2003**, 726. (c) Mirica, L. M.; Vance, M.; Rudd, D. J.; Hedman, B.; Hodgson, K. O.; Solomon, E. I.; Stack, T. D. P. *Science* **2005**, *308*, 1890. (d) Op't Holt, B. T.; Vance, M. A.; Mirica, L. M.; Heppner, D. E.; Stack, T. D. P.; Solomon, E. I. *J. Am. Chem. Soc.* **2009**, *131*, 6421. (e) Esguerra, K. V. N.; Fall, Y.; Lumb, J.-P. *Angew. Chem. Int. Ed.* **2014**, *53*, 5877. (f) Itoh, S.; Kumei, H.; Taki, M.; Nagatomo, S.; Kitagawa, T.; Fukuzumi, S. *J. Am. Chem. Soc.* **2001**, *123*, 6708. (g) Hoffmann, A.; Citek, C.; Binder, S.; Goos, A.; Rübhausen, M.; Troeppner, O.; Ivanović-Burmazović, I.; Wasinger, E. C.; Stack, T. D. P.; Herres-Pawlis, S. *Angew. Chem. Int. Ed.* **2013**, *52*, 5398. (h) Arnold, A.; Metzinger, R.; Limberg, C. *Chem. Eur. J.* **2015**, *21*, 1198.
(10) (a) Mirica, L. M.; Ottenwaelder, X.; Stack, T. D. P. *Chem. Rev.* **2004**, *104*, 1013. (b) Lewis, E. A.; Tolman, W. B. *Chem. Rev.* **2004**, *104*, 1047.
(11) (a) Magdziak, D.; Rodriguez, A. A.; Van De Water, R. W.; Pettus, T. R. R. *Org. Lett.* **2002**, *4*, 285. (b) Finley, K. T. *Quinones as Synthones*, In *The Quinonoid Compounds (1988)*; John Wiley & Sons: New York, **2010**, Chap. 11, 537. (c) Fishwick, C. W. G.; Jones, D. W. *ortho-Quinonoid Compounds*, In *The Quinonoid Compounds (1988)*; John Wiley & Sons: New York, **2010**, Chap. 9, 403. (d) Uyanik, M.; Mutsuga, T.; Ishihara, K. *Molecules* **2012**, *17*, 8604.
(12) Verma, P.; Weir, J.; Mirica, L.; Stack, T. D. P. *Inorg. Chem.* **2011**, *50*, 9816.
(13) Corey, E. J.; Achiwa, K. *J. Am. Chem. Soc.* **1969**, *91*, 1429.
(14) Osako, T.; Ohkubo, K.; Taki, M.; Tachi, Y.; Fukuzumi, S.; Itoh, S. *J. Am. Chem. Soc.* **2003**, *125*, 11027.
(15) Armstrong, D. R.; Cameron, C.; Nonhebel, D. C.; Perkins, P. G. *J. Chem. Soc., Perkin Trans. 2* **1983**, 587.
(16) Askari, M. S.; Esguerra, K. V. N.; Lumb, J.-P.; Ottenwaelder, X. *Inorg. Chem.* **2015**, *54*, 8665.
(17) (a) Marín-Zamora, M. E.; Rojas-Melgarejo, F.; García-Cánovas, F.; García-Ruiz, P. A. *J. Biotechnol.* **2009**, *139*, 163. (b) Guazzaroni, M.; Crestini, C.; Saladino, R. *Bioorg. Med. Chem.* **2012**, *20*, 157.
(18) Müller, E.; Mayer, R.; Narr, B.; Rieker, A.; Scheffler, K. *Justus Liebigs Ann. Chem.* **1961**, *645*, 25.
(19) Meier, H.; Schneider, H.-P.; Rieker, A.; Hitchcock, P. B. *Angew. Chem.* **1978**, *90*, 128.
(20) Rayne, S.; Forest, K. *Struct. Chem.* **2011**, *22*, 615.
(21) (a) Hewgill, F. R.; La Greca, B.; Legge, F.; Roga, P. E. *J. Chem. Soc., Perkin Trans. 1* **1983**, 131. (b) Rayne, S.; Sasaki, R.; Wan, P. *Photochem. Photobiol. Sci.* **2005**, *4*, 876. (c) Haack, P.; Kärgel, A.; Greco, C.; Dokic, J.; Braun, B.; Pfaff, F. F.; Mebs, S.; Ray, K.; Limberg, C. *J. Am. Chem. Soc.* **2013**, *135*, 16148.
(22) CCDC 1527150 (**3**), 1527151 (**7**), and 1527152 (**7a**) contain the supplementary crystallographic data for this paper. The data can be obtained free of charge from The Cambridge Crystallographic Data Centre via www.ccdc.cam.ac.uk/getstructures.
(23) $157.50 CAD/mg at the time of writing, Sigma-Aldrich catalogue #PH000046.
(24) Izawa, Y.; Pun, D.; Stahl, S. S. *Science* **2011**, *333*, 209.
(25) (a) Xia, S.; Gan, L.; Wang, K.; Li, Z.; Ma, D. *J. Am. Chem. Soc.* **2016**, *138*, 13493. (b) Chen, Y.; Zou, Y.; Sun, H.-Y.; Liu, X.-K.; Xiao, C.-F.; Sun, J.; He, S.-J.; Li, J. *Synthesis* **2011**, 217. (c) Chen, J.; Yuan, T.; Hao, W.; Cai, M. *Catal. Commun.* **2011**, *12*, 1463. (d) Wang, Y.; Zhou, C.; Wang, R. *Green Chem.* **2015**, *17*, 3910. (e) Elder, J. W.; Mariella, R. P. *Can. J. Chem.* **1963**, *41*, 1653.
(26) (a) Norberg, A. M.; Smith, M. R. III.; Maleczka, R. E. Jr. *Synthesis* **2011**, 857. (b) Maleczka, R. E.; Shi, F.; Holmes, D.; Smith, M. R. *J. Am. Chem. Soc.* **2003**, *125*, 7792.
(27) **Synthesis of 3 via Borylation and Oxidation**
NOTE – caution should always be taken when performing large-scale oxidations. Risks are minimized here by carefully controlling the rate of addition of Oxone®.
A 250 mL round-bottom flask equipped with a Teflon-coated magnetic stir bar was charged with **8** (26.9 g, 100 mmol, 1 equiv), Mg turnings (3.65 g, 150 mmol, 1.5 equiv), and a piece of I_2 crystal. The reaction was put under N_2, and dry, degassed THF (100 mL) was added to the flask. The mixture was stirred at r.t. until initiation of the reaction was visible. An ice bath was used for cooling the reaction in the event that the temperature rose too high. In a separate 500 mL round-bottom flask equipped with a Teflon-coated magnetic stir bar, $B(OMe)_3$ (21.2 mL, 200 mmol, 2 equiv) was added via syringe, followed by the addition of THF (100 mL). The solution was cooled to 0 °C using an ice bath, and stirred under N_2. The THF solution of the Grignard reagent was transferred to the cooled flask containing the $B(OMe)_3$ solution via cannula. Once the addition was complete, the reaction was stirred vigorously and warmed back to r.t. for 2 h. The reaction was then cooled back down to 0 °C and quenched by the addition of 1 M HCl (80 mL). The solution was extracted using EtOAc (3 × 200 mL), the organic layers were combined, and dried over $MgSO_4$. The crude reaction mixture was concentrated in vacuo to give a yellow solid. This was transferred to a 2 L round-bottom flask equipped with a Teflon-coated magnetic stir bar, re-dissolved in acetone (600 mL), and an aq solution of Oxone® (61.5 g, 200 mmol, 2 equiv in 600 mL H_2O) was added dropwise at r.t. over 1 h, and stirred for another 7 min. The reaction was then carefully quenched by the addition of sat. aq $NaHSO_3$ (200 mL), and concentrated in vacuo to remove most of the acetone. The crude reaction mixture was extracted with CH_2Cl_2 (3 × 200 mL), the organic layers were combined, dried over $MgSO_4$, and concentrated in vacuo to obtain a yellow solid. Flash column chromatography (hexanes–EtOAc, gradient from 100:0 to 90:10) yielded **3** as a yellow solid (18.7 g, 90% before recrystallization), and it was recrystallized from hexanes (50 mL) to yield pure **8** as colorless crystals (16.5 g, 80%). ^1H NMR (500 MHz, $CDCl_3$): δ = 7.00 (t, J = 1.7 Hz, 1 H), 6.68 (d, J = 1.7 Hz, 2 H), 4.52 (br s, 1 H), 1.30 (s, 18 H) ppm. ^{13}C NMR (125 MHz, $CDCl_3$): δ = 154.8, 152.7, 115.2, 110.0, 34.9, 31.5 ppm. Analytical data matches that of the commercially available material.
(28) Xu, B.; Lumb, J.-P.; Arndtsen, B. A. *Angew. Chem. Int. Ed.* **2015**, *54*, 4208.